

Contents lists available at ScienceDirect

# **International Journal of Engineering Science**

journal homepage: www.elsevier.com/locate/ijengsci



Full length article

# Development of a versatile indoor framework for the measurement of tyre compound friction and wear

Andrea Genovese, Guido Napolitano Dell'Annunziata, Emanuele Lenzi, Aleksandr Sakhnevych, Francesco Timpone, Flavio Farroni

University of Naples Federico II, Department of Industrial Engineering, Via Claudio 21, Naples, 80125, Italy

# ARTICLE INFO

# Keywords: Friction Rubber Tyre tread Linear friction tester Specimen conditioning Surface rubberisation

# ABSTRACT

Maximising tyre performance requires balancing conflicting targets, grip, wear resistance, and rolling efficiency, while accelerating development. In this context, tribological characterisation at compound level supports faster prototyping and reduces reliance on full-scale testing. Although standards for rubber friction testing exist, they are rarely followed in literature. and procedures are often underreported. This work addresses that gap by presenting the complete development of an experimental framework for rubber friction and wear testing, with particular focus on tyre tread compound, from the definition of functional requirements to the design of a novel linear friction tester and the implementation of a robust testing methodology. The Ground Rubber Interface Performance (GRIP) tester was designed for high versatility and cost-effectiveness. A key feature is the open-access architecture, which allows practical surface management and rapid retooling. A custom back-heating system ensures uniform specimen temperature even under varying test conditions. The methodology focuses on critical but overlooked aspects: specimen conditioning, surface rubberisation, and temperature control. Case studies demonstrate the repeatability of results and the system's sensitivity to key input parameters. Additional tests confirm the platform's adaptability to non-tyre tribological applications.

### 1. Introduction

In the automotive industry, tyre performance maximisation is a relevant topic that affects all aspects of road transport and motorsport alike. On one hand, tyres play a central role in vehicle manoeuvrability and road user safety, as they are required to maximise both longitudinal and lateral acceleration under a wide range of environmental conditions (Farroni & Sakhnevych, 2022; Sakhnevych, 2022). On the other hand, tyre performance is increasingly tied to environmental and sustainability concerns. Low rolling resistance contributes to reduced fuel consumption and greenhouse gas emissions (Barrand & Bokar, 2008), while high wear resistance is essential for minimising non-exhaust particulate matter emissions (Baensch-Baltruschat, Kocher, Stock, & Reifferscheid, 2020; Zhang et al., 2023). These objectives are inherently conflicting due to the bulk viscoelasticity and the surface chemistry of the tread compound. The same hysteretic losses that aid in generating grip over wet surfaces (Persson, 2001; Tabor, 1960) are opposed to the wheel free rolling (Hall & Moreland, 2001); at the same time, the tangential interactions opposing slip can lead to material consumption, either through fatigue or tensile failure (Grosch, 2008).

E-mail addresses: andrea.genovese2@unina.it (A. Genovese), guido.napolitanodellannunziata@unina.it (G. Napolitano Dell'Annunziata), emanuele.lenzi@unina.it (E. Lenzi), aleksandr.sakhnevych@unina.it (A. Sakhnevych), francesco.timpone@unina.it (F. Timpone), flavio.farroni@unina.it (F. Farroni).

https://doi.org/10.1016/j.ijengsci.2025.104402

Received 18 August 2025; Received in revised form 13 October 2025; Accepted 13 October 2025

Available online 17 October 2025

0020-7225/© 2025 The Authors. Published by Elsevier Ltd. This is an open access article under the CC BY-NC-ND license (http://creativecommons.org/licenses/by-nc-nd/4.0/).

<sup>\*</sup> Corresponding author.

Rubber tribological phenomena have been extensively addressed over the last century, yet an accepted unified theory has not been reached due to the complexity that non-linearities and external factors bring (Myshkin, Petrokovets, & Kovalev, 2005; Xu, Sheng, Zhou, & Persson, 2025). Many authors have pointed out the difficulty of predicting polymers behaviour due to unresolved factors, such as the role of chemical interactions (Fukahori, Gabriel, Liang, & Busfield, 2020; Tiwari, Miyashita, Espallargas, & Persson, 2018), the presence of a third body in the interaction (Harsha, Tewari, & Venkatraman, 2003), or non-linear viscoelasticity (Le Gal, Yang, & Klüppel, 2005) to name a few. To explore these effects in a controlled and reproducible manner, laboratory tribometers are essential. By systematically isolating key parameters, such as surface roughness, contact pressure, and temperature, they offer a practical route to deepen understanding and support compound development beyond what purely analytical or numerical tools can currently achieve. However, the definition of a reliable and repeatable testing procedure remains a critical issue. Existing standards for rubber friction characterisation (Rubber — Determination of frictional properties, 2005; Standard guide for measuring and reporting friction coefficients, 2018) provide general guidance but do not adequately reflect real tyre operating conditions. Consequently, most experimental studies diverge from these specifications but rarely provide a systematic methodology for doing so (Lahayne, Eberhardsteiner, & Reihsner, 2009; Lorenz, Persson, Dieluweit, & Tada, 2011; Rosu, Elias-Birembaux, Lebon, Lind, & Wangenheim, 2016).

This paper introduces an integrated experimental methodology for the tribological characterisation of rubber compounds across a wide range of operating conditions, from high-load truck tyres to high-temperature motorsport applications. The entire process of definition of the framework is presented: it begins with the identification of functional requirements based on tribological theory, continues through the design and development of a dedicated test rig, the Ground Rubber Interface Performance (GRIP) tester, and is concluded with the definition of a robust and repeatable testing procedure.

The development of the GRIP tester and its associated testing procedure addresses two critical challenges in rubber friction characterisation: the need for practical, flexible hardware that supports surface maintenance and accurate thermal control, and the definition of a repeatable and physically consistent methodology to ensure reliability of the results.

The key innovations and advantages of the proposed framework are:

- 1. The GRIP tester features a novel open-access architecture, allowing quick and direct access to the counter surface. This facilitates cleaning operations to remove worn particles from the contact area, allowing wear testing without the use of anti-smearing powder. Furthermore, it allows quick retooling of the specimen to increase testing efficiency.
- To ensure isothermal conditions without the need for a climate chamber, a custom heating element is embedded into the specimen holder and paired with infrared temperature sensors, offering precise and uniform thermal control. The work chamber is thus always safely accessible.
- 3. The testing protocol explicitly includes specimen conditioning and surface cleaning as critical steps. These practices ensure that multiple specimens can be tested on the same track without loss of information or reliability.
- 4. The full procedure is validated through repeated measurements under varying operating conditions, showing low dispersion and high sensitivity to control parameters.
- 5. The design allows adaptation to different specimen geometries and contact materials, extending applicability to non-rubber tribological investigations.

The article is structured as follows: Section 2 derives the functional requirements from fundamental principles of rubber friction and wear. The implementation of these requirements into a versatile design is described in Section 3. Lastly, the developed experimental procedure is presented in Section 4 through several case studies. The capabilities of the platform are demonstrated, not only within tyre applications, but also across a broader range of tribological context.

#### 2. From state of the art analysis to functional requirement definition

The development of an integrated experimental framework begins with the definition of functional requirements, hereafter referred to as FR. These requirements guide the design of a testing system capable of reproducing the wide range of conditions relevant to rubber tribology.

Rubber friction and wear are governed by the viscoelastic behaviour of elastomers (Grosch & Schallamach, 1966; Lancaster, 1968; Mané et al., 2013; Pal, Das, Rajasekar, Pal, & Das, 2009). Their long, entangled molecular chains enable large reversible deformations, but the delayed recovery dissipates energy and strongly influences mechanical response. Reinforcing fillers further modify this behaviour: while they improve stiffness and strength, they also introduce additional non-linearities even at small strains (De & White, 2001; Payne, 1962; Zhang, 2004). Altogether, these features make the response of rubber highly sensitive to bulk temperature, loading frequency, and strain amplitude.

Friction in rubber is widely recognised to result from two main mechanisms: interfacial adhesion, due to chemical interactions at the contact, and bulk hysteresis, related to the cyclic loading induced by surface roughness (Schallamach, 1958). Grosch (1963) showed that friction can be directly linked to rubber rheology, constructing master curves by applying the time–temperature superposition principle (Williams, Landel, & Ferry, 1955). Wear processes are likewise distinct from those of elastic solids. Rubber wear arises from three competing mechanisms: abrasion, when local stresses exceed material strength; fatigue, associated with repeated loading that produces characteristic Schallamach waves; and smearing, involving oxidative transfer layers on the counter surface under milder conditions (Gent & Pulford, 1983; Schallamach, 1968). Moore (1980) proposed that adhesion-driven friction is primarily linked to abrasion and smearing, while hysteresis governs fatigue wear.

Table 1
Summary of functional requirements.

	•	
Label	Requirement description	
FR-1	Control the parameters that influence viscoelastic response: load, sliding speed, and temperature.	
FR-2	Ensure isothermal conditions during testing or quantify thermal increase.	
FR-3	Enable mounting of different surface types and geometries.	
FR-4	Allow easy access to the contact surface for cleaning and interventions.	
FR-5	Operate reliably under dry, dusty, or wet environmental conditions.	

From these insights, a first requirement can be identified: a test system must control the key parameters governing viscoelastic response: normal load, sliding speed, and bulk temperature (FR1). These parameters are interdependent: frictional heating modifies the viscoelastic response, creating feedback where the friction coefficient evolves during sliding (Persson, 2006b). To achieve stable and repeatable measurements, the system must therefore ensure isothermal conditions during testing or be able to quantify the thermal increase (FR2).

The other side of the tribological equation is the counter-surface against which rubber slides, particularly in terms of roughness, chemical composition, and the presence of any contact modifiers, e.g. dust, water, lubricants, or smeared layers. Many engineering surfaces are rough across multiple length scales, and this multiscale character strongly influences the actual contact area that the rubber can establish with the substrate (Avolio, Lenzi, Dell'Annunziata, Ruffini, & Genovese, 2024; Jacobs, Junge, & Pastewka, 2017; Persson, Albohr, Tartaglino, Volokitin, & Tosatti, 2004). Consequently, friction and wear behaviour are closely tied to surface topography (Farroni, Stefanelli, Dell'Annunziata, & Timpone, 2025; Persson, 2006a). Different roughness levels can reduce or suppress adhesion (Afferrante, Violano, & Dini, 2023; Tiwari, Wang, & Persson, 2020), while Persson (2001) and Kluppel and Heinrich (2000) modelled how asperities deform the rubber during sliding, giving rise to hysteretic dissipation.

Surface sharpness is often cited as the most relevant parameter to govern the wear mechanisms. Although the literature is not decisive in the quantitative definition of sharpness, it has been linked to a shift in wear behaviour: abrasion is commonly associated with pointier asperities, where stress concentrations can lead to cutting and material removal, while smoother asperities are more often linked to adhesive wear and smearing phenomena (Emami & Khaleghian, 2019; Muhr & Roberts, 1992; Shen, Dong, Zhang, Meng, & Peng, 2016). To study such a variety of surfaces, the machine must allow for high modularity in surface mounting, accommodating different shapes and sizes (FR3). Most notably, a system capable of accommodating samples from specific outdoor tracks would enable the development of robust correlations between indoor rubber friction and outdoor tyre grip.

Beyond the geometry and roughness of the surface, the presence of contaminants acts as a contact modifier. For instance, in motorsport applications a smeared rubber layer deposited on the track is known to enhance grip (Tiwari, Miyashita, & Persson, 2021). The smeared layer also modifies the wear response of the rubber, acting as a lubricant (Briscoe & Sinha, 2002). To avoid these influences, two strategies can be adopted. On one hand, applying a fine powder can help prevent the build-up of oxidised rubber, as it acts as a cleaning agent, though it also introduces a third body into the contact (Stachowiak & Stachowiak, 2001). On the other hand, it is necessary to mechanically clean the surface at predetermined intervals. Additionally, the presence of water or other lubricants can inhibit adhesion and smear (Hatanaka et al., 2025) and limit the penetration of rubber into surface asperities (Persson, 2001). These considerations lead to two final requirements: the counter-surface must be easily accessible to allow frequent cleaning (FR-4), and the test rig must operate reliably in wet and dusty environments (FR-5).

A summary of the functional requirements derived from the previous considerations is provided in Table 1.

Having defined the functional requirements, it is useful to examine how existing tribometers, both in the literature and international standards, address these needs. These devices can generally be grouped into two categories: continuous-motion and intermittent-motion systems (Brown, 2006; Genovese, D'Angelo, Sakhnevych, & Farroni, 2020; Rubber, vulcanized or thermoplastic — Abrasion testing — Guidance, 2005). Continuous-motion testers involve a specimen either rolling or sliding against a rotating element, such as a drum or a disk. These configurations are advantageous for wear studies, as they allow for uninterrupted operation over extended distances, but limit the choice of surfaces that can be used (Gent & Nah, 1996; Pal et al., 2010; Salehi, Noordermeer, Reuvekamp, Dierkes, & Blume, 2019). Cylindrical drums require flexible coverings, such as sandpaper or diamond-coated cloths, while disks can accommodate stiffer materials like asphalt but are limited in rotational speed due to centrifugal effects. Intermittentmotion testers, on the other hand, typically involve linear sliding of the specimen against a flat, stationary surface. This category includes devices such as the British Pendulum (Ciaravola et al., 2017; Liu, Fwa, & Choo, 2004), simple and cost-effective though limited in regulations, and Linear Friction Testers (LFTs), which have become the de facto standard in rubber friction characterisation due to their parameter control and surface flexibility (Lahayne et al., 2009; Rosu et al., 2016; Rubber — Determination of frictional properties, 2005). LFTs offer the advantage of high versatility in tribological testing. They can accommodate various test surfaces, including asphalt tiles, and allow quick replacement to manage polishing or debris accumulation. They are also better suited to specimens with varying shapes and sizes. Their main drawback lies in wear testing, where the limited sliding distance and intermittent motion can make such tests time-consuming. However, proper design and automated controls can mitigate these constraints.

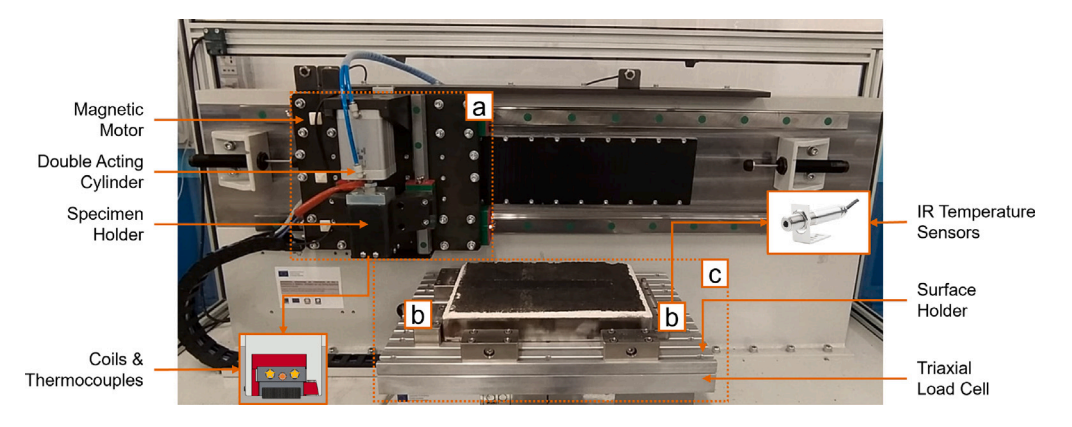


Fig. 1. GRIP linear friction tester general scheme: (a) specimen assembly, (b) IR temperature sensors, (c) surface assembly.

#### 3. GRIP tester design and raw data analysis

Building on the functional requirements outlined above, the Ground Rubber Interface Performance (GRIP) tester was designed as a modular linear friction tester capable of addressing a broad range of experimental needs within a cost-effective architecture.

The main design choice lies in the absence of a thermally controlled chamber. While this presents the challenge of heating the specimen and maintaining a constant temperature (the adopted solution will be discussed in the next Section), it offers key advantages: rapid and easy access to the working area, continuous visual monitoring, reduced retooling time, and the ability to perform interventions on the road surface, such as cleaning, powder application, or lubricant addition, without interrupting the workflow (FR-4). This open architecture represents the main novelty from other devices described in the literature (Lorenz et al., 2011; O'Neill, 2021; Rantonen, Tuononen, & Sainio, 2012; Ripka, Gäbel, & Wangenheim, 2009). The scheme of the device is shown in Fig. 1.

The specimen assembly (Fig. 1a) is composed of a specimen holder, a double-acting cylinder and a magnetic motor. The specimen holder houses a heated aluminium plate monitored by a thermocouple. The rubber specimen is glued onto a  $35 \times 35 \text{ mm}^2$  aluminium base, which accommodates various specimen geometries up to that footprint. The base gets mounted directly against the heating element with thermal paste, forming a system that ensures heating from the bottom of the specimen to the surface. The thermal mass of the holder helps in retaining high temperatures even without insulating the test chamber, guaranteeing small temperature fluctuations. The double-acting cylinder and the magnetic motor control the movement of the specimen during the runs. The vertical motion of the specimen is controlled by the pneumatic cylinder, which regulates contact pressure via a manometer. The pneumatic setup also helps dampen vibrations induced by surface texture, resulting in smoother normal force profiles. Meanwhile, the magnetic motor drives the rubber specimen along the surface at either constant velocity or controlled acceleration, enabling both stationary and transient testing conditions. The real-time position of the motor is monitored, allowing the manipulation of sliding distances. This subsystem addresses FR-1, by ensuring controlled load, speed, and temperature.

To meet FR-2, a pair of infrared temperature sensors (Fig. 1b) monitor the initial and final surface temperature of the rubber, controlling the thermal range of the test. Combined with bottom-side heating, this setup promotes a uniform temperature distribution across the specimen, avoiding the use of a thermally controlled chamber.

Finally, the surface assembly (Fig. 1c) includes a triaxial load cell and a modular surface holder. The load cell is fully sealed to enable operation under a variety of environmental conditions (FR-5). It measures the contact forces throughout the run and is mechanically balanced to prevent measurement errors caused by off-centre specimen positioning. A T-slot aluminium plate is mounted on the load cell, and several sliding retainer blocks can be repositioned to clamp surfaces of different shapes and sizes (FR-3), up to  $400 \times 250 \text{ mm}^2$ . Table 2 summarises the nameplate data for all systems discussed.

With the system set up, the testing and data acquisition procedure is fully automated. After specifying the desired initial temperature, sliding velocity, and contact pressure, the machine performs a three-step sequence: (1) an initial temperature reading, (2) execution of the test run, and (3) a final temperature reading. The initial temperature acts as the primary control parameter: each run begins only when the specimen's temperature falls within a predefined tolerance of the target value. During the test, the system continuously records the motor position and speed, as well as the vertical  $(F_z)$  and longitudinal  $(F_x)$  contact forces, as illustrated in Fig. 2(a). Normal and tangential forces are sampled at 500 Hz and pre-processed with a low-pass Butterworth filter to suppress high-frequency background noise. The cut-off frequency is selected as a function of the sliding velocity and average wavelength of the surface, to avoid removal of significant signal components.

The test sequence is divided into four phases:

- 1. O-A: the specimen is moved into the starting position when the desired temperature is reached;
- A-B: the vertical load is applied, followed by a dwell time before initiating sliding. The dwell time is typically a fraction of a second but can be adjusted to investigate the influence of relaxation on static friction (Barquins & Roberts, 1986; Persson et al., 2003);

**Table 2**GRIP components datasheet.

Component	Quantity	Range	Unit of measurement
Motor	Speed Acceleration Longitudinal force	[0.001, 1] [0.008, 8] [7.5, 3000]	m/s m/s² N
Cylinder	Vertical force	[70, 1570]	N
Temperature Control	Temperature	[T <sub>amb</sub> , 80]	°C
Load Cell	Longitudinal force Lateral force Vertical force	[-2.5, 2.5] [-1, 1] [0, 2]	kN kN kN

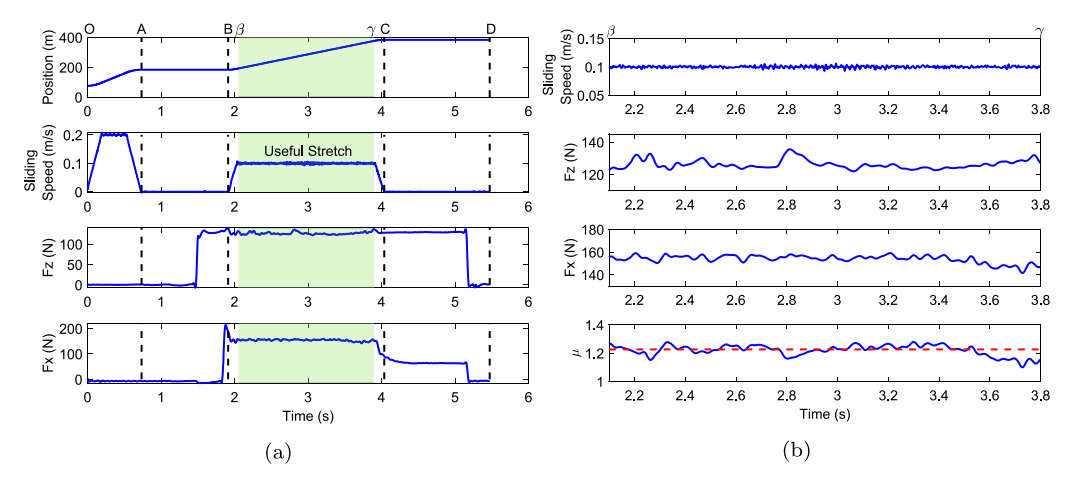


**Fig. 2.** Raw data acquisition and friction coefficient calculation. (a) Acquired test data: motor position and speed, vertical  $(F_z)$  and longitudinal  $(F_z)$  contact forces; (b) Extraction of the useful stretch and dynamic friction estimation.

3. **B-C**: this is the main testing phase. In the most common configuration of stationary testing, it consists of an acceleration phase, a constant velocity phase, and a deceleration phase. Point B corresponds to the instant when static friction is overcome and sliding begins; this allows the extraction of the static friction coefficient as in Eq. (1).

$$\mu_{static} = F_{x,peak} / F_{z,peak} \tag{1}$$

Following the acceleration phase, a section of the run where the sliding speed remains constant  $(\beta-\gamma)$  is identified. This stretch, referred to as the useful stretch (US), defines the portion of data used for calculating the dynamic friction coefficient (Fig. 2(b)). Specifically, the normal and longitudinal forces are extracted over the US, their element-wise ratio is computed, and the median value of this ratio (indicated by the red dashed line) is taken as the dynamic friction coefficient (Eq. (2)).

$$\mu_{dynamic} = median(F_{x,US}/F_{z,US}) \tag{2}$$

4. **C-D**: the test concludes. The specimen is lifted and moved to the final position for temperature measurement. Both the initial and final temperature values are then computed as the arithmetic mean of the raw measurements.

In addition to individual friction tests, the machine supports an automated repetition mode suitable for wear testing. In this configuration, the B–C segment and the final temperature reading are automatically repeated for a user-defined number of cycles. The specimen is weighed before and after the full sequence with an external precision scale (resolution 0.0001 g) to determine mass loss, while the evolution of friction and surface temperature is logged for each cycle. Measuring mass after every single run would introduce inefficiencies due to repeated specimen remounting, and the wear accumulated in one cycle is generally too small to be detected with sufficient accuracy. For this reason, multiple cycles are clustered before weighing, both to accumulate a measurable mass loss and to overcome the initial thermal transient, during which the specimen progressively heats up and stabilises. This approach provides a practical compromise consistent with the nature of wear testing, while still allowing correlation between thermal build-up, frictional response, and wear behaviour.

#### 4. Experimental methodology and results

A robust experimental protocol completes the proposed framework, with a focus on measurement consistency and sensitivity to relevant differences in material composition and operating conditions. The methodology is validated through a series of case

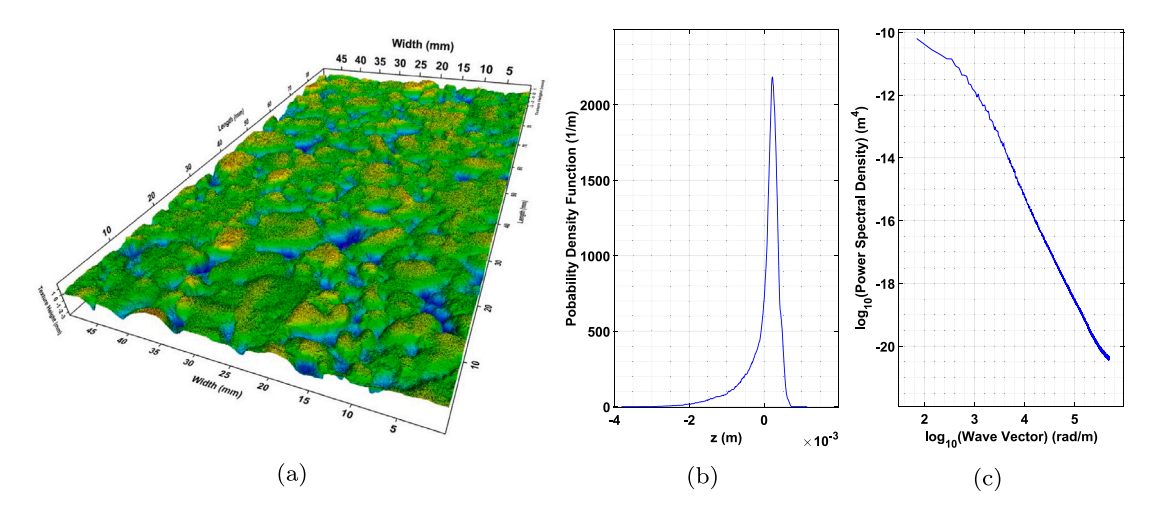


Fig. 3. Surface roughness acquisition and roughness parameters calculation. (a) 3D surface scan; (b) Probability distribution function of heights; (c) Power spectral density of heights.

studies that collectively aim to demonstrate repeatable results and physically consistent trends in response to controlled parameter changes. First, the role of compound formulation and specimen conditioning is examined to highlight the platform's sensitivity at the material scale. Next, the influence of surface roughness and contact modifiers is explored, followed by tests that isolate the effects of sliding speed, pressure, and temperature, and their cross-dependencies. Finally, additional capabilities of the GRIP tester are illustrated, demonstrating its adaptability to broader tribological contexts. This sequence was deliberately chosen to reflect the relative impact of each factor on measurement reliability, with conditioning introduced first as the prerequisite to interpreting the effects of subsequent parameters.

The presented case studies involve three commercially available tyre tread compounds selected to represent a wide range of applications: a motorsport rubber (referred to as M-compound), optimised for peak performance at elevated temperatures; a truck rubber (T-compound), formulated for extended durability under high loads; and a summer passenger car rubber (P-compound), designed as a balance for all around use. The materials were supplied by industrial partners in the form of vulcanised rubber slabs of dimensions  $300 \times 300 \times 4$  mm<sup>3</sup>. The slabs were then processed by die-cutting  $25 \times 25 \times 4$  mm<sup>3</sup> specimens. Unless otherwise specified, the reference counter surface was a dense-graded asphalt tile, representative of typical outdoor operative conditions on non-draining roads. Surface roughness was characterised using an optical profilometer based on laser triangulation (AMES LTS 9400HD). As shown in Fig. 3(a), the 3D acquisition was performed over an area of  $50 \times 90$  mm<sup>2</sup> along the line followed by the specimen during sliding. This window was chosen to fully encompass the specimen footprint, with tolerance for positioning errors, while being long enough to avoid artefacts from local surface imperfections. From the 3D reconstruction, roughness indicators can be extracted. For completeness, Figs. 3(b) and 3(c) report the probability distribution function and the power spectral density of the asphalt tile, which some authors consider the most comprehensive descriptors of surface roughness (Persson, 2023).

#### 4.1. Specimen conditioning, compound sensitivity and measurements reliability

To ensure the reliability of the friction measurements, newly prepared specimens must undergo a conditioning phase before the actual testing campaign. In fact, virgin samples exhibit a transient phase in which their frictional response evolves over successive runs, showing inconsistent values with a clear trend. During conditioning, the progressive wear of the specimen alters the initially flat contact surface, leading to the formation of a geometry adapted to the working conditions. After a sufficient number of cycles, the specimen typically exhibits a worn leading edge and an intact trailing edge due to the shearing deformation it undergoes. This geometry better conforms to the applied load, stabilising the frictional response. In addition, cyclic loading induces mechanical softening phenomena that influence the tribological response (Mullins, 1969). At present, no systematic studies have been published that define how conditioning procedures should vary depending on compound formulation, and therefore, no standardised guidelines can be established. Some authors have cited the implementation of a conditioning procedure for friction testing (Emami, Khaleghian, Bezek, & Taheri, 2020; Ripka et al., 2009; Rosu et al., 2016; Shams Kondori & Taheri, 2022) mostly done to remove "sharp edges", but these works do not explain the rationale nor the conditions behind their procedure. Indeed, experimental experience suggests that loading history may be an influential parameter in the final friction response, thus, to ensure comparability, all specimens should be conditioned in the same manner. The specific parameters of the conditioning procedure may vary depending on the objectives of the test campaign. In general, to account for the effects of viscoelastic relaxation, it is advisable to condition all specimens at the maximum expected normal load, thereby reducing the likelihood of additional mechanical relaxation during subsequent tests. Sliding speeds should remain relatively low to avoid excessive wear. In this work, a specimen is considered properly conditioned when five consecutive tests yield a friction coefficient with less than 2% deviation and no evident trend in the evolution curve.

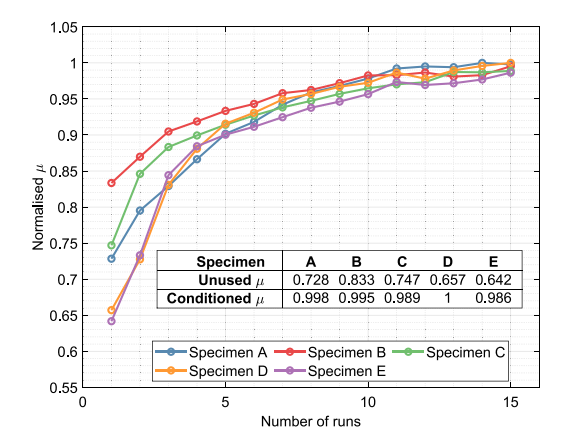


Fig. 4. Friction response evolution of five summer passenger car tread compound specimens during conditioning runs on an asphalt tile.

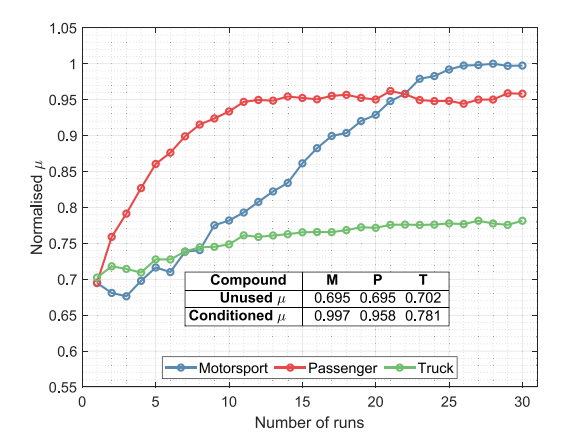


Fig. 5. Friction response evolution of three different tread compound specimens during conditioning runs on an asphalt tile.

Fig. 4 illustrates the conditioning under repeated testing of five new P-compound specimens. The friction coefficient was normalised as a function of the maximum obtained value to highlight the deviation between specimens. The conditioning procedure was performed under the following reference conditions: contact pressure of 0.20 MPa, sliding speed of 0.10 m/s, temperature of 30 °C, and a sliding distance of 200 mm per run. These conditions were chosen as a common operating region for all three compounds, even though they may not fully represent the optimal working range of each material. Initially, the unused specimens exhibit varied friction levels, which rapidly evolve over successive runs and converge towards a common steady-state value. After sufficient conditioning, the final friction coefficients across compounds show a maximum deviation below 2%. The table included in the figure reports the unused  $\mu$  and conditioned  $\mu$ , which are respectively the normalised friction value at the start and at the end of the transient phase.

The differences between the three compounds can already be observed by comparing their evolution during conditioning, as shown in Fig. 5, where the frictional behaviour aligns with each material intended application. The truck compound, formulated for durability under high loads and long mileage, evolves quite slowly under these mild conditions with a relatively modest increase in grip. Similarly, the motorsport compound, designed to deliver high grip within a narrow and typically much hotter temperature window, also evolves gradually but reaches the highest friction coefficient. Conversely, the passenger compound, for which these conditions are more suitable, quickly reaches a stable performance.

For the actual testing, a comparison was conducted under the same conditions, across a sliding speed range spanning two orders of magnitude from 0.001 m/s to 0.10 m/s. As a general testing methodology, a single specimen is used across the full velocity range, starting from the slowest speed and progressing to the highest. The specimen is replaced whenever the vertical load or counter-surface is changed. These choices are motived by two key considerations: wear progression is minimised at low velocities due to negligible thermal build-up, allowing a more stable initial condition; keeping the same load and temperature across the full speed range isolates the specimen's loading history, enabling direct comparison across all test points. To ensure statistical reliability while maintaining efficiency, each condition is repeated five times. The dynamic friction coefficient is extracted from the useful stretch of each run, and the final result is taken as the median of the five repetitions, as discussed in Lenzi, Farroni, Sakhnevych, Timpone, and Genovese (2024). Fig. 6(a) shows the resulting friction curves for the three compounds. The relative ranking remains

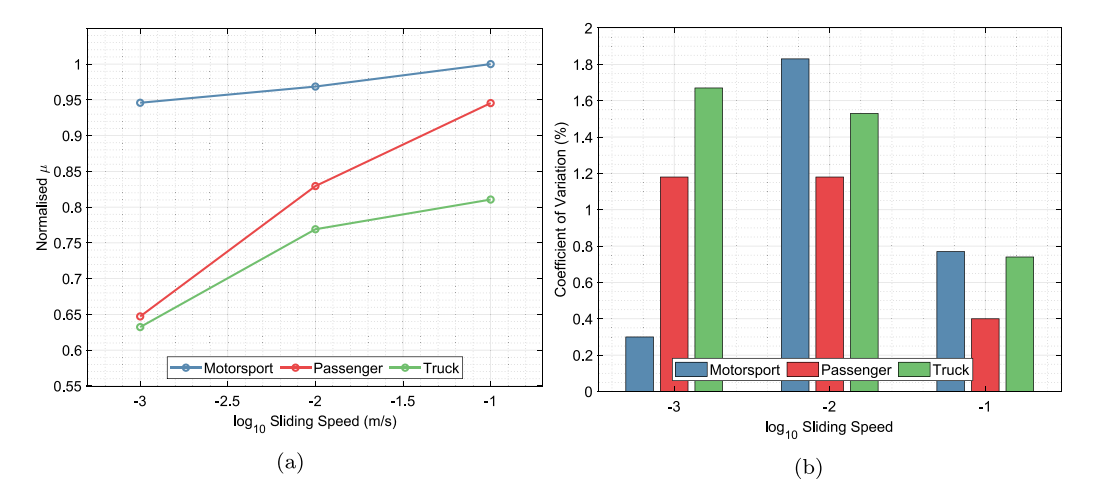


Fig. 6. Friction response comparison (a) and measurement repeatability (b) of three different tread compounds tested on an asphalt tile.

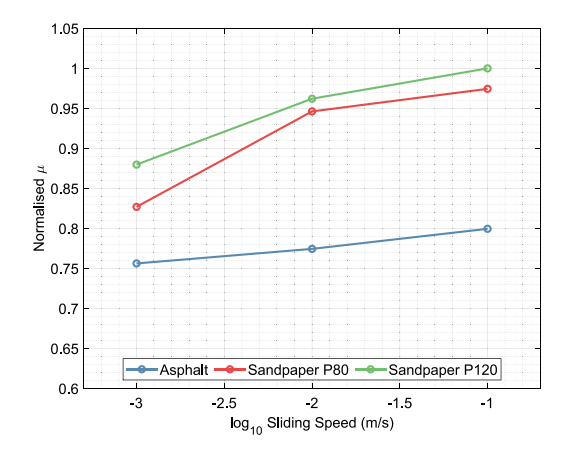


Fig. 7. Friction response of a motorsport tread compound on three different counter-surfaces.

consistent with expectations: the motorsport compound exhibits the highest grip, followed by the passenger compound, with the truck compound performing the lowest. These findings prove the sensitivity of the procedure even under non-ideal conditions. To assess measurement repeatability, Fig. 6(b) reports the coefficient of variation (CV) across the five repetitions, computed as the ratio between the standard deviation and the median friction value. The combination of low deviations between different specimens (less than 2% as shown in Fig. 4) and good repeatability across multiple runs is necessary to ensure the reliability of the measurements.

#### 4.2. Surface roughness and contact modifiers

With the conditioning protocol and data aggregation established, attention shifts to the influence of surface roughness and debris accumulation. Fig. 7 compares three different surfaces tested with the motorsport tyre tread compound. To emphasise the influence of roughness, the reference asphalt tile was compared with two sandpapers of different grit sizes: P80 and P120. Sandpaper is commonly used in friction and wear testing as it is readily available and consistent in texture and composition across different sheets (Budinski, 2007). The comparison tests were performed under the following reference conditions: contact pressure of 0.20 MPa, sliding speed ranging from 0.001 to 0.10 m/s, temperature of 30 °C, and a sliding distance of 200 mm per run.

The results show an inverse correlation between the friction coefficient and the macroscopic coarseness of the surface. The smoothest sandpaper (P120) offers the highest grip, followed by the slightly rougher P80, whereas the significantly coarser asphalt tile ranks lowest. This trend may be explained by how surface roughness affects the formation of the real contact area. Rubber has a limited ability to fully conform to the surface asperities, thus the actual area of contact is typically smaller than the nominal one (Farroni et al., 2025; Le Gal & Klüppel, 2007; Persson, 2006a). Smoother surfaces allow for a more effective indentation by the rubber, resulting in a larger real contact area and higher friction levels. Additionally, differences in chemical composition between the asphalt and the sandpapers may alter the adhesive friction contribution, further increasing the overall differences.

Consequently, the presence of any contact modifier can lead to variations in the measured friction response. A prime example is the accumulation of rubber residue on the surface during repeated testing. Fig. 8 shows the effects of rubberisation on the asphalt

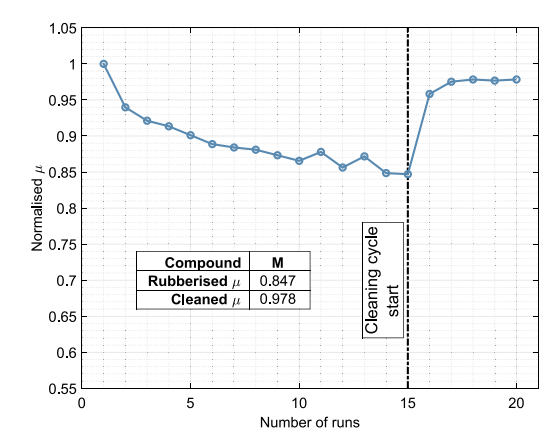


Fig. 8. Friction response evolution of a motorsport tread compound specimen during repeated runs on an asphalt tile. The first fifteen runs are performed consecutively to accumulate rubber residue on the surface. The final five runs are each preceded by a mechanical cleaning of the surface.

during repeated testing of the motorsport tyre tread compound. The tests were performed under the following reference conditions: contact pressure of 0.20 MPa, sliding speed of 0.10 m/s, temperature of 30 °C, and a sliding distance of 200 mm per run. The conditioned specimen underwent fifteen consecutive runs starting from a washed and dried surface, after which a cleaning cycle was introduced. In this phase, five additional runs were conducted, each preceded by a simple mechanical cleaning using a stiff-bristle brush and a natural rubber eraser. The table included in the Figure reports the rubberised and cleaned  $\mu$ , corresponding respectively to the normalised friction value at the fifteenth run, prior the cleaning cycle starting, and at the last run of the cleaning cycle. The data show that the accumulation of rubber on the surface strongly affects friction, with a strong decreasing trend over repeated runs. This effect is proved by the fact that the mechanical cleaning restores the friction coefficient within 2%–3% of its initial value. These results stress the importance of ensuring rapid and simple access to the counter surface for cleaning procedures to obtain stable and repeatable results. In this context, a closed-chamber setup becomes a limitation: since surface cleaning may be required before every run, either auxiliary in-situ cleaning systems must be integrated, adding complexity and cost, or the machine must automatically unload the specimen, perform a cleaning cycle with a dedicated rubber element, and reload the test specimen. While feasible, this approach significantly reduces testing throughput compared to an open-access configuration, where manual cleaning can be performed quickly and directly.

#### 4.3. Sliding speed, pressure, and temperature cross-influences

The final part of the procedure focuses on control parameters that are often interdependent: sliding speed, bulk temperature, and contact pressure. These factors are difficult to isolate, as increases in pressure or sliding speed typically lead to higher frictional power and, consequently, to increased specimen temperature. A robust test setup, paired with a reliable experimental procedure, should minimise such cross-influences to study one parameter at a time.

To demonstrate this capability, two case studies have been conducted. The first explores the combined effect of sliding speed and contact pressure on the thermal rise of the specimen. Fig. 9 shows the friction response and mean surface temperature of the truck tread compound. Six contact pressures, distributed over an order of magnitude from 0.15 to 1.50 MPa, and ten sliding speeds, spanning three orders of magnitude from 0.002 to 1 m/s, were selected for the study. The truck compound was chosen because it is the most adapt material to reach extremely high levels of contact pressures. Fig. 9(a) shows a marked increase in friction coefficient as load decreases, with a nearly 50% drop between the lowest and highest pressures. This behaviour is documented in the literature where it is typically associated to two main effects: the sub-linear increase of real contact area with load, until saturation to its nominal value, and the thermal rise due to higher energy dissipation at higher loads (Bush, Gibson, & Thomas, 1975; Fortunato et al., 2017). It is therefore necessary to avoid a marked thermal increase to isolate the pure pressure effect. Fig. 9(b) shows the average test temperature, evaluated as the arithmetic mean between the initial and final surface temperature of the rubber, compared to a target temperature of 30 °C. At low speeds (below 0.01 m/s) the temperature appears mostly independent of the contact pressure. At higher sliding speeds, particularly above 0.50 m/s, the contribution of the frictional heating becomes more pronounced. This confirms that an increase in pressure and speed is necessary to cause a substantial thermal rise. Nonetheless, by appropriately regulating the sliding distance, the thermal spike can be kept within acceptable bounds under most conditions. These data underline the importance of measuring the temperature of the specimen and carefully regulating its movements to be able to separate interest parameters from each other.

The second case study demonstrates the ability of the GRIP machine to control the specimen temperature without a thermally controlled chamber. Fig. 10 shows the friction response and the surface temperature evolution of the motorsport tread compound. Four nominal temperatures, ranging from 50 to 80 °C, and three sliding speeds, spanning two order of magnitude, were selected. The motorsport compound was chosen due to its intended use in high-temperature conditions.

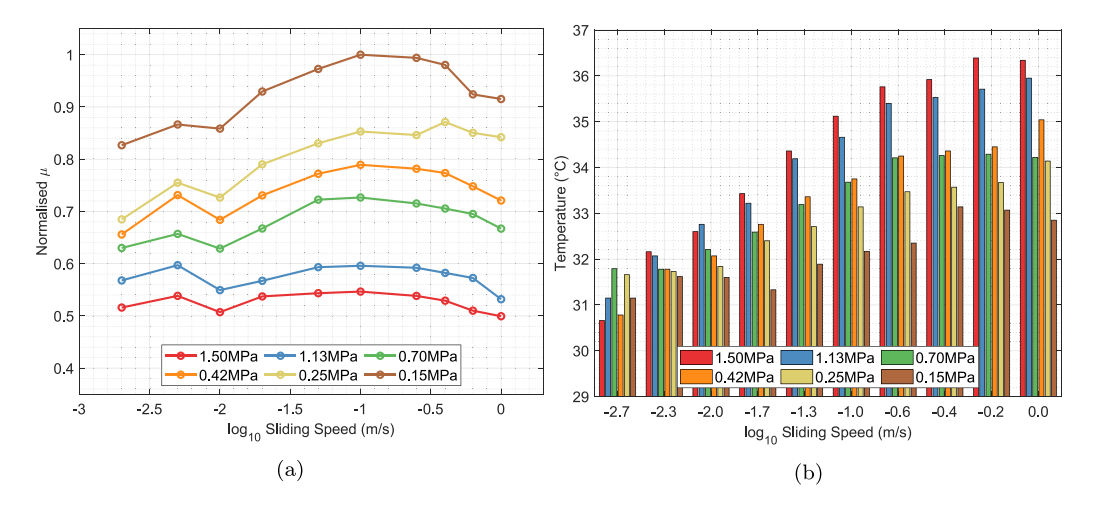


Fig. 9. Friction response (a) and mean temperature (b) of a truck tread compound tested on an asphalt tile under varying loads and sliding speeds.

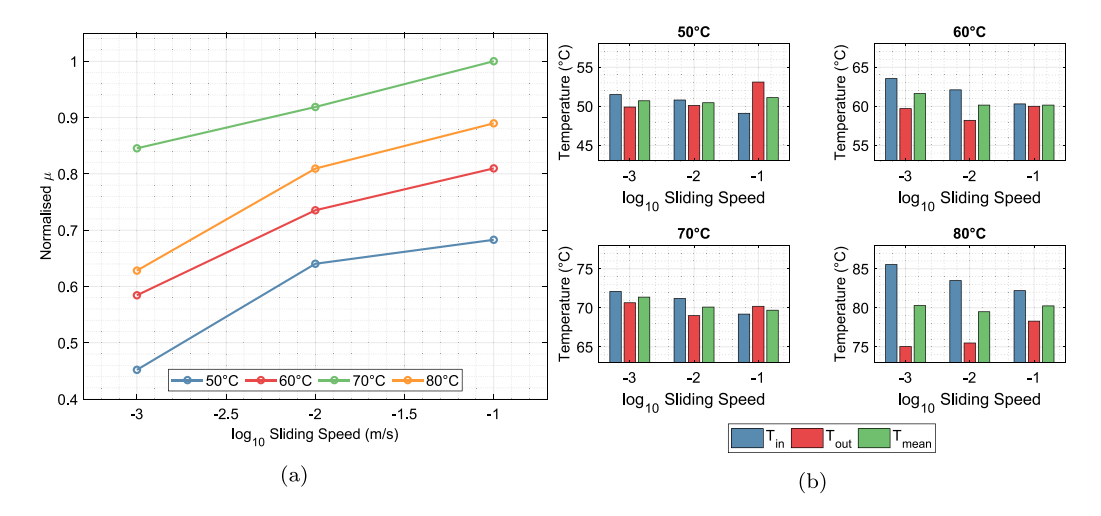


Fig. 10. Friction response (a) and surface temperature evolution (b) of a motorsport tread compound tested on an asphalt tile under varying temperatures and sliding speeds.

Fig. 10(a) shows the performance variation of the compound under varying temperature. The material exhibits a marked increase in performance at 70 °C, highlighting the importance of the correct temperature windows when employing high-performance materials. Fig. 10(b) shows the comparison between input  $(T_{in})$ , output  $(T_{out})$ , and mean  $(T_{mean})$  surface temperature across the test conditions. As expected, the absence of a thermally controlled chamber is more obvious the higher the nominal temperature and the slower is the sliding speed. It should be noted that, although the worst condition exhibits a  $\pm 5$  °C deviation from the nominal temperature, this does not necessarily reflect the internal thermal state of the specimen. Due to the low thermal conductivity of rubber and the short-duration of the tests the bulk of the material is likely to remain near the set-point temperature. This helps explain why a clear difference in friction response is still observed between tests conducted at 70 °C and 80 °C.

These results confirm that the experimental setup is capable of decoupling the effects of speed, pressure, and temperature, enabling targeted investigations even in the absence of a thermal chamber.

#### 4.4. Additional capabilities

Lastly, to remark the aforementioned versatility that the GRIP tester provides beyond rubber–road contact, a case study involving truck tarpaulin systems is presented. These systems use a motorised tarpaulin that slides along metal guide rails through a set of polymeric sliding pads, which are consumable components. The objective of the study was to evaluate whether different surface finishes on the guide rails could reduce sliding friction and thereby extend the service life of the pads. To carry out these tests, a dedicated adapter (Fig. 11a) was 3D-printed to mount commercial sliding pads onto the GRIP specimen holder (Fig. 11b). The

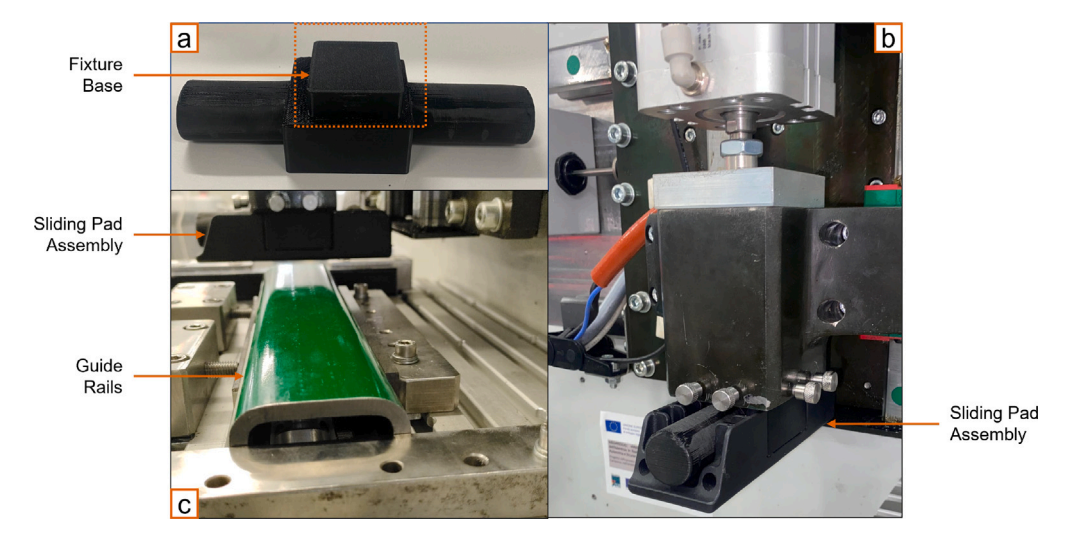


Fig. 11. Adaptation of a truck tarpaulin slider system for friction testing: (a) 3D-printed adapter for slider mounting; (b) Complete slider assembly installed on the GRIP tester; (c) Clamping of the guiding rail.

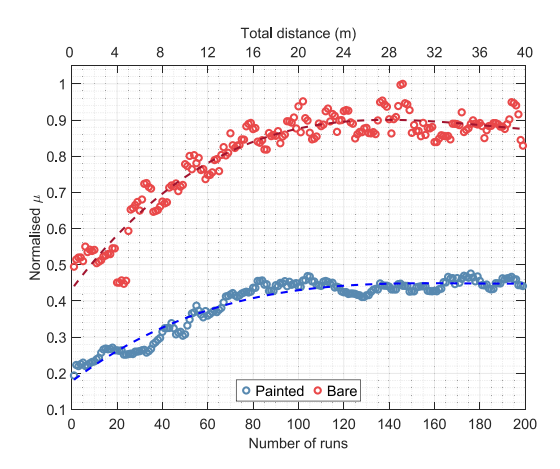


Fig. 12. Friction response of a polymeric sliding pad on guide rails with different surface finishes.

modular clamping system of the tester enabled direct installation of a segment of guide rail (Fig. 11c). Two types of rails were tested: bare aluminium and aluminium coated with abrasion resistant paint.

Test parameters were selected to reflect real operating conditions: a vertical load of 100 N, a sliding speed of 0.10 m/s, and a sliding distance of 200 mm per run, repeated for 200 cycles. Fig. 12 shows the friction response of both configurations. A run-in phase is observed during the first 100 cycles, as the sliding pads conform to the guide geometry. After stabilisation, the coated rail demonstrates a substantial reduction in friction: approximately 50% lower than the bare aluminium rail.

This application further illustrates how the experimental framework can be adapted to diverse contact materials and industrial use cases with minimal modifications.

#### 4.5. Main findings

The results presented in this study demonstrate that the GRIP tester, combined with a well-defined experimental methodology, can deliver reliable and physically consistent measurements. Beyond reproducing established tribological trends, the framework highlights distinctive features that improve both the robustness and the versatility of laboratory testing. In particular, the main findings can be summarised as follows:

Proper conditioning is essential to ensure a stable response across different specimens. As shown in Fig. 4, once the
leading/trailing edge geometry is established and the compound has undergone enough loading cycles, the specimens converge
towards a consistent behaviour that can be reliably compared. In this stable regime, the GRIP tester achieves low variability,

with coefficients of variation below 2% across compounds and test conditions (Fig. 6(b)), allowing repeated runs to be performed with high confidence.

- The modular design enables mounting of different counter-surfaces for direct comparison, while the open chamber facilitates rapid and effective cleaning. This has a dual effect: on one hand, it ensures repeatability between consecutive runs (friction values within 2% on clean surfaces as shown in Fig. 8), and on the other, it allows meaningful comparison of different specimens over long testing sequences without residues compromising the results. In contrast, uncleaned, rubberised surfaces can produce a drop exceeding 15%. Unlike conventional setups that rely on anti-smearing powders, the open chamber allows rapid manual cleaning, removing this additional variable while maintaining efficiency.
- The back-heating system provides a simple and inexpensive alternative to a climatic chamber, enabling high-temperature testing while preserving operator access to the working chamber. Although heat dissipation to the counter-surface limits extreme conditions, the system still produces clearly categorised results and allows direct monitoring of pressure–speed–temperature interactions.
- The adopted mounting solutions extend the applicability of the apparatus beyond rubber friction. By accommodating a wide variety of specimen geometries and counter-surfaces, the GRIP tester supports tribological investigations on a broader class of materials and interfaces. This versatility makes the device not only a tool for compound development but also a methodological platform for studying fundamental tribological mechanisms in controlled laboratory conditions.

#### 5. Conclusion

This paper presented the development of a complete experimental framework for the tribological characterisation of rubber compounds, encompassing the definition of functional requirements, the design of the GRIP linear friction tester, and the formulation of a robust and repeatable testing methodology. A review of the current literature on rubber friction and wear informed the definition of key functional requirements. These guided the design of the GRIP linear friction tester, with a specific focus on versatility, cost-effectiveness, and ease of use. Unlike existing devices in the literature, the GRIP tester introduces a novel open-access architecture specifically designed to allow rapid and direct interventions on the contact surface. This choice enables practical retooling and surface cleaning between runs, a critical need for accurate testing that is rarely addressed in conventional setups. Although this design forgoes a thermally controlled chamber, a custom back-heating system embedded in the specimen holder, coupled with infrared monitoring, ensures adequate temperature control across the specimen volume while keeping system complexity and cost low. In perspective, this accessibility also opens the possibility of systematically investigating the role of anti-smearing powders in wear testing. The open chamber can be quickly accessed for frequent cleaning, making it feasible to compare tests performed with and without powders, in an approach that would be impractical in closed-chamber configurations.

The proposed experimental methodology addresses several key aspects often neglected in literature. Conditioning procedures, test sequencing, and cleaning protocols are clearly defined, based on physical reasoning and supported by experimental evidence. Case studies show that the methodology achieves high repeatability and clearly resolves differences due to compound formulation, surface roughness, and operational parameters. The results follow expected physical trends and demonstrate that thermal drift can be effectively managed within the open setup. A natural extension of this work will be to systematically investigate the influence of load and thermal history on conditioning, with the aim of defining standardised procedures applicable across compounds.

Finally, the modular nature of the GRIP tester allows for adaptation beyond tyre applications, supporting rapid prototyping and broader tribological research. Overall, this work demonstrates that a methodology-driven approach to machine design, combined with clear and validated testing procedures, can offer a reliable platform for compound development and friction analysis.

## CRediT authorship contribution statement

Andrea Genovese: Writing – review & editing, Writing – original draft, Supervision, Project administration, Methodology, Investigation, Conceptualization. Guido Napolitano Dell'Annunziata: Writing – review & editing, Writing – original draft, Visualization, Software, Methodology, Formal analysis. Emanuele Lenzi: Writing – review & editing, Writing – original draft, Visualization, Software, Methodology, Investigation, Data curation. Aleksandr Sakhnevych: Validation, Software, Funding acquisition, Data curation, Conceptualization. Francesco Timpone: Visualization, Supervision, Investigation, Funding acquisition, Conceptualization. Flavio Farroni: Validation, Supervision, Funding acquisition, Formal analysis, Conceptualization.

#### Declaration of competing interest

The authors declare that they have no known competing financial interests or personal relationships that could have appeared to influence the work reported in this paper.

#### Data availability

The authors do not have permission to share data.

#### References

Afferrante, L., Violano, G., & Dini, D. (2023). How does roughness kill adhesion? Journal of the Mechanics and Physics of Solids, 181, Article 105465.

Avolio, S., Lenzi, E., Dell'Annunziata, G. N., Ruffini, M., & Genovese, A. (2024). Topography measurements analysis between road surfaces and their silicone replicas. In *International tribology symposium of iFToMM* (pp. 357–366). Springer.

Baensch-Baltruschat, B., Kocher, B., Stock, F., & Reifferscheid, G. (2020). Tyre and road wear particles (TRWP)-A review of generation, properties, emissions, human health risk, ecotoxicity, and fate in the environment. Science of the Total Environment, 733, Article 137823.

Barquins, M., & Roberts, A. (1986). Rubber friction variation with rate and temperature: some new observations. *Journal of Physics D (Applied Physics)*, 19(4), 547

Barrand, J., & Bokar, J. (2008). Reducing tire rolling resistance to save fuel and lower emissions. SAE International Journal of Passenger Cars-Mechanical Systems, 1(2008-01-0154), 9-17.

Briscoe, B. J., & Sinha, S. (2002). Wear of polymers. Proceedings of the Institution of Mechanical Engineers, Part J: Journal of Engineering Tribology, 216(6), 401–413. Brown, R. (2006). Physical testing of rubber. Springer Science & Business Media.

Budinski, K. G. (2007). Guide to friction, wear and erosion testing. ASTM international West Conshohocken, PA.

Bush, A., Gibson, R., & Thomas, T. (1975). The elastic contact of a rough surface. Wear, 35(1), 87-111.

Ciaravola, V., Farroni, F., Fortunato, G., Russo, M., Russo, R., Sakhnevych, A., et al. (2017). An evolved version of the british pendulum tester for the experimental investigation of contact between tire tread and rough surfaces. *Engineering Letters*, 25(1).

De, S. K., & White, J. R. (2001). Rubber technologist's handbook: Vol. 1, iSmithers Rapra Publishing.

Emami, A., & Khaleghian, S. (2019). Investigation of tribological behavior of styrene-butadiene rubber compound on asphalt-like surfaces. *Tribology International*, 136, 487–495.

Emami, A., Khaleghian, S., Bezek, T., & Taheri, S. (2020). Design and development of a new portable test setup to study friction and wear. Proceedings of the Institution of Mechanical Engineers, Part J: Journal of Engineering Tribology, 234(5), 730–742.

Farroni, F., & Sakhnevych, A. (2022). Tire multiphysical modeling for the analysis of thermal and wear sensitivity on vehicle objective dynamics and racing performances. Simulation Modelling Practice and Theory, 117, Article 102517.

Farroni, F., Stefanelli, R., Dell'Annunziata, G. N., & Timpone, F. (2025). Impact of the tire/road local contact area on tire friction, with a novel approach based on Greenwood-Williamson theory and validation in both laboratory and outdoor racing environments. *Tribology International*, Article 110772.

Fortunato, G., Ciaravola, V., Furno, A., Scaraggi, M., Lorenz, B., & Persson, B. N. (2017). Dependency of rubber friction on normal force or load: theory and experiment. *Tire Science and Technology*, 45(1), 25–54.

Fukahori, Y., Gabriel, P., Liang, H., & Busfield, J. (2020). A new generalized philosophy and theory for rubber friction and wear. Wear, 446, Article 203166.

Genovese, A., D'Angelo, G. A., Sakhnevych, A., & Farroni, F. (2020). Review on friction and wear test rigs: An overview on the state of the art in tyre tread friction evaluation. *Lubricants*, 8(9), 91.

Gent, A., & Nah, C. (1996). Abrasion of rubber by a blade abrader: effect of blade sharpness and test temperature for selected compounds. *Rubber Chemistry and Technology*, 69(5), 819–833.

Gent, A., & Pulford, C. (1983). Mechanisms of rubber abrasion. Journal of Applied Polymer Science, 28(3), 943-960.

Grosch, K. (1963). The relation between the friction and visco-elastic properties of rubber. Proceedings of the Royal Society of London. Series A. Mathematical and Physical Sciences, 274(1356), 21–39.

Grosch, K. (2008). Rubber abrasion and tire wear. Rubber Chemistry and Technology, 81(3), 470-505.

Grosch, K., & Schallamach, A. (1966). Relation between abrasion and strength of rubber. Rubber Chemistry and Technology, 39(2), 287-305.

Hall, D. E., & Moreland, J. C. (2001). Fundamentals of rolling resistance. Rubber Chemistry and Technology, 74(3), 525-539.

Harsha, A., Tewari, U., & Venkatraman, B. (2003). Three-body abrasive wear behaviour of polyaryletherketone composites. Wear, 254(7-8), 680-692.

Hatanaka, S., Ogawa, Y., Okubo, H., Hanzawa, K., Kajiki, R., Yamaguchi, K., et al. (2025). Correlation between friction and wear of rubber: An experimental approach based on the disconnections of stribeck curves. Wear, 562, Article 205623.

Jacobs, T. D., Junge, T., & Pastewka, L. (2017). Quantitative characterization of surface topography using spectral analysis. Surface Topography: Metrology and Properties. 5(1). Article 013001.

Kluppel, M., & Heinrich, G. (2000). Rubber friction on self-affine road tracks. Rubber Chemistry and Technology, 73(4), 578-606.

Lahayne, O., Eberhardsteiner, J., & Reihsner, R. (2009). Tribological investigations carried out by a linear friction tester. Transactions of FAMENA, 33(2).

Lancaster, J. (1968). Relationships between the wear of polymers and their mechanical properties. In Proceedings of the institution of mechanical engineers, conference proceedings: Vol. 183, (pp. 98–106). SAGE Publications Sage UK: London, England.

Le Gal, A., & Klüppel, M. (2007). Investigation and modelling of rubber stationary friction on rough surfaces. *Journal of Physics: Condensed Matter*, 20(1), Article 015007.

Le Gal, A., Yang, X., & Klüppel, M. (2005). Evaluation of sliding friction and contact mechanics of elastomers based on dynamic-mechanical analysis. *Journal of Chemical Physics*, 123(1).

Lenzi, E., Farroni, F., Sakhnevych, A., Timpone, F., & Genovese, A. (2024). Laboratory linear friction tester: Design and results. In *International tribology symposium* of iFToMM (pp. 23–30). Springer.

Liu, Y., Fwa, T., & Choo, Y. (2004). Effect of surface macrotexture on skid resistance measurements by the British pendulum test. *Journal of Testing and Evaluation*, 32(4), 304–309.

Lorenz, B., Persson, B., Dieluweit, S., & Tada, T. (2011). Rubber friction: comparison of theory with experiment. The European Physical Journal E, 34, 1-11.

Mané, Z., Loubet, J.-L., Guerret, C., Guy, L., Sanseau, O., Odoni, L., et al. (2013). A new rotary tribometer to study the wear of reinforced rubber materials. Wear, 306(1-2), 149-160.

Moore, D. F. (1980). Friction and wear in rubbers and tyres. Wear, 61(2), 273-282.

Muhr, A., & Roberts, A. (1992). Rubber abrasion and wear. Wear, 158(1-2), 213-228.

Mullins, L. (1969). Softening of rubber by deformation. Rubber Chemistry and Technology, 42(1), 339-362.

Myshkin, N., Petrokovets, M., & Kovalev, A. (2005). Tribology of polymers: Adhesion, friction, wear, and mass-transfer. *Tribology International*, 38(11–12), 910–921.

O'Neill, A. (2021). Predicting tyre behaviour on different road surfaces (Ph.D. thesis), University of Surrey.

Pal, K., Das, T., Rajasekar, R., Pal, S. K., & Das, C. K. (2009). Wear characteristics of styrene butadiene rubber/natural rubber blends with varying carbon blacks by DIN abrader and mining rock surfaces. *Journal of Applied Polymer Science*, 111(1), 348–357.

Pal, K., Rajasekar, R., Kang, D. J., Zhang, Z. X., Pal, S. K., Das, C. K., et al. (2010). Effect of fillers on natural rubber/high styrene rubber blends with nano silica: morphology and wear. *Materials & Design*, 31(2), 677–686.

Payne, A. R. (1962). The dynamic properties of carbon black-loaded natural rubber vulcanizates. Part i. Journal of Applied Polymer Science, 6(19), 57-63.

Persson, B. N. (2001). Theory of rubber friction and contact mechanics. Journal of Chemical Physics, 115(8), 3840-3861.

Persson, B. N. (2006a). Contact mechanics for randomly rough surfaces. Surface Science Reports, 61(4), 201-227.

Persson, B. N. (2006b). Rubber friction: role of the flash temperature. Journal of Physics: Condensed Matter, 18(32), 7789.

Persson, B. (2023). On the use of surface roughness parameters. Tribology Letters, 71(2), 29.

Persson, B. N., Albohr, O., Mancosu, F., Peveri, V., Samoilov, V., & Sivebæk, I. M. (2003). On the nature of the static friction, kinetic friction and creep. Wear, 254(9), 835–851.

Persson, B. N., Albohr, O., Tartaglino, U., Volokitin, A. I., & Tosatti, E. (2004). On the nature of surface roughness with application to contact mechanics, sealing, rubberfriction and adhesion. *Journal of Physics: Condensed Matter*, 17(1), R1.

Rantonen, M., Tuononen, A. J., & Sainio, P. (2012). Measuring stud and rubber friction on ice under laboratory conditions. *International Journal of Vehicle Systems Modelling and Testing*, 7(2), 194–207.

Ripka, S., Gäbel, G., & Wangenheim, M. (2009). Dynamics of a siped tire tread block—experiment and simulation. *Tire Science and Technology*, 37(4), 323–339. Rosu, I., Elias-Birembaux, H. L., Lebon, F., Lind, H., & Wangenheim, M. (2016). Experimental and numerical simulation of the dynamic frictional contact between

(2005). Rubber — Determination of frictional properties: Vol. 2005, Geneva, CH: International Organization for Standardization.

(2005). Rubber, vulcanized or thermoplastic — Abrasion testing — Guidance: Vol. 2023, Geneva, CH: International Organization for Standardization.

Sakhnevych, A. (2022). Multiphysical MF-based tyre modelling and parametrisation for vehicle setup and control strategies optimisation. *Vehicle System Dynamics*, 60(10), 3462–3483.

Salehi, M., Noordermeer, J. W., Reuvekamp, L. A., Dierkes, W. K., & Blume, A. (2019). Measuring rubber friction using a laboratory abrasion tester (LAT100) to predict car tire dry ABS braking. *Tribology International*, 131, 191–199.

Schallamach, A. (1958). Friction and abrasion of rubber. Wear, 1(5), 384-417.

an aircraft tire rubber and a rough surface. Lubricants, 4(3), 29.

Schallamach, A. (1968). Abrasion, fatigue, and smearing of rubber. Journal of Applied Polymer Science, 12(2), 281-293.

Shams Kondori, M., & Taheri, S. (2022). Linear friction tester design and validation. Proceedings of the Institution of Mechanical Engineers, Part J: Journal of Engineering Tribology, 236(5), 856–866.

Shen, M.-X., Dong, F., Zhang, Z.-X., Meng, X.-K., & Peng, X.-D. (2016). Effect of abrasive size on friction and wear characteristics of nitrile butadiene rubber (NBR) in two-body abrasion. *Tribology International*, 103, 1–11.

Stachowiak, G., & Stachowiak, G. (2001). The effects of particle characteristics on three-body abrasive wear. Wear, 249(3-4), 201-207.

(2018). Standard guide for measuring and reporting friction coefficients. West Conshohocken, PA, USA: ASTM International.

Tabor, D. (1960). Hysteresis losses in the friction of lubricated rubber. Rubber Chemistry and Technology, 33(1), 142-150.

Tiwari, A., Miyashita, N., Espallargas, N., & Persson, B. N. (2018). Rubber friction: The contribution from the area of real contact. *Journal of Chemical Physics*, 148(22).

Tiwari, A., Miyashita, N., & Persson, B. (2021). Rubber wear and the role of transfer films on rubber friction on hard rough substrates. *Tribology Letters*, 69, 1–12.

Tiwari, A., Wang, J., & Persson, B. (2020). Adhesion paradox: Why adhesion is usually not observed for macroscopic solids. *Physical Review E*, 102(4), Article 042803.

Williams, M. L., Landel, R. F., & Ferry, J. D. (1955). The temperature dependence of relaxation mechanisms in amorphous polymers and other glass-forming liquids. *Journal of the American Chemical Society*, 77(14), 3701–3707.

Xu, R., Sheng, W., Zhou, F., & Persson, B. (2025). Rubber wear: History, mechanisms, and perspectives. arXiv preprint arXiv:2503.19494.

Zhang, S.-W. (2004). Tribology of elastomers: Vol. 47, Elsevier.

Zhang, M., Yin, H., Tan, J., Wang, X., Yang, Z., Hao, L., et al. (2023). A comprehensive review of tyre wear particles: Formation, measurements, properties, and influencing factors. Atmospheric Environment, 297, Article 119597.